Journal of Asian Earth Sciences 35 (2009) 502–515

Contents lists available at ScienceDirect

Journal of Asian Earth Sciences

journal homepage: www.elsevier.com/locate/jaes

Petrogenesis of extension-related alkaline volcanism in Karaburhan (Sivrihisar–Eskisehir), NW Anatolia, Turkey

Ender Sarıfakıoğlu [a,*], Hayrettin Özen [a], Chris Hall [b]

[a] Department of Geology, The General Directorate of Mineral Research and Exploration, 06620 Ankara, Turkey
[b] Department of Geological Sciences, University of Michigan, Ann Arbor, MI 48109-1009, USA

ARTICLE INFO

Article history:
Received 6 May 2008
Received in revised form 16 March 2009
Accepted 19 March 2009

Keywords:
Alkaline volcanic rocks
Geochemical characteristics
Fluids
Subduction component
Turkey

ABSTRACT

Alkaline lavas were erupted as phonolites and trachytes around Karaburhan (Sivrihisar–Eskisehir, NW Anatolia) within the Izmir–Ankara–Erzincan suture zone. These volcanic rocks were emplaced as domes, close and parallel to the ophiolite thrust line. According to $^{40}Ar/^{39}Ar$ geochronological analyses of sanidine crystals from the phonolites, the age of the alkaline volcanics is 25 Ma (Late Oligocene–Early Miocene).

The flow-textured phonolites are porphyritic and consist mainly of sanidine, clinopyroxene, and feldspathoid crystals. The clinopyroxenes show compositional zoning, with aegirine ($Na_{0.82-0.96}Fe^{+3}_{0.68-0.83}$) rims and aegirine–augite cores (containing calcium, magnesium, and Fe^{+2}). Some aegirine–augites are replaced with sodium-, calcium-, and magnesium-rich amphibole (hastingsite). Feldspathoid (hauyne) crystals enriched with elemental Na and Ca have been almost completely altered to zeolite and carbonate minerals. The fine-grained trachytes with a trachytic texture consist of feldspar (oligoclase and sanidine) phenocrystals and clinopyroxene microphenocrystals within a groundmass made up largely of alkali feldspar microlites.

Although there are some differences in their element patterns, the phonolites and trachytes exhibit enrichment in LILEs (Sr, K, Rb, Ba, Th) and LREEs (La, Ce, Pr, Nd) and negative anomalies in Nb and Ta. These geochemical characteristics indicate a lithospheric mantle enriched by fluids extracted from the subduction component. In addition, the high $^{87}Sr/^{86}Sr$ (0.706358–0.708052) and low $^{143}Nd/^{144}Nd$ (0.512546–0.512646) isotope concentrations of the alkaline lavas reflect a mantle source that has undergone metasomatism by subduction-derived fluids. Petrogenetic modeling indicates that the alkaline lavas generated from the subduction-modified lithospheric mantle have undergone assimilation, fractional crystallization, and crustal contamination, acquiring high Pb, Ba, Rb, and Sr contents and Pb isotopic compositions during their ascent through the thickened crust in an extensional setting.

1. Introduction

In Anatolia, the microcontinents separated by the northern and southern branches of the Neo-Tethyan Ocean collided as a result of the closure of this ocean. This major event, which caused the neotectonic regime in Turkey, gave rise to Tertiary volcanism, which progressed from west to east across the area (Şengör and Yılmaz, 1981; Yılmaz, 1990).

In NW Turkey, the northern branch of the Neo-Tethyan Ocean, the Izmir–Ankara–Erzincan Ocean, between the Sakarya Continent to the north and the Anatolide–Tauride Platform to the south, was closed by the collision of the two continents during the Upper Cretaceous–Early Eocene (Harris et al., 1994; Okay et al., 2001). Following this event was a N–S shortening and thickening of the lithosphere, accompanied by the development of E–W trending strike-slip faults, leading to a N–S extension in the investigated area (Fig. 1).

In the Galatia Volcanic Province situated 80 km north of the investigated area, Early Miocene trachyandesites and trachydacites were derived from a lithospheric mantle source metasomatically enriched by fluids above the subduction zone, and Late Miocene alkali basalts formed from the asthenospheric mantle (Wilson et al., 1997). Temel (2001) postulated that the alkali basaltic and trachytic rocks of the Oglakci (Sivrihisar, Eskisehir) region are products of post-collisional Miocene alkaline volcanism having a within-plate character in the extensional tectonic regime. The Quaternary products of Cappadocia in the Central Anatolian volcanic province, ranging from acid/intermediate to mafic composition, are interpreted as having been derived from lithospheric mantle sources that included remnants of subducted material (Türkecan et al., 2004).

* Corresponding author. Tel.: +90 312 287 34 30/1626; fax: +90 312 285 42 71.
E-mail address: esarifakioglu@yahoo.com (E. Sarıfakıoğlu).

1367-9120/$ - see front matter © 2009 Elsevier Ltd. All rights reserved.
doi:10.1016/j.jseaes.2009.03.002

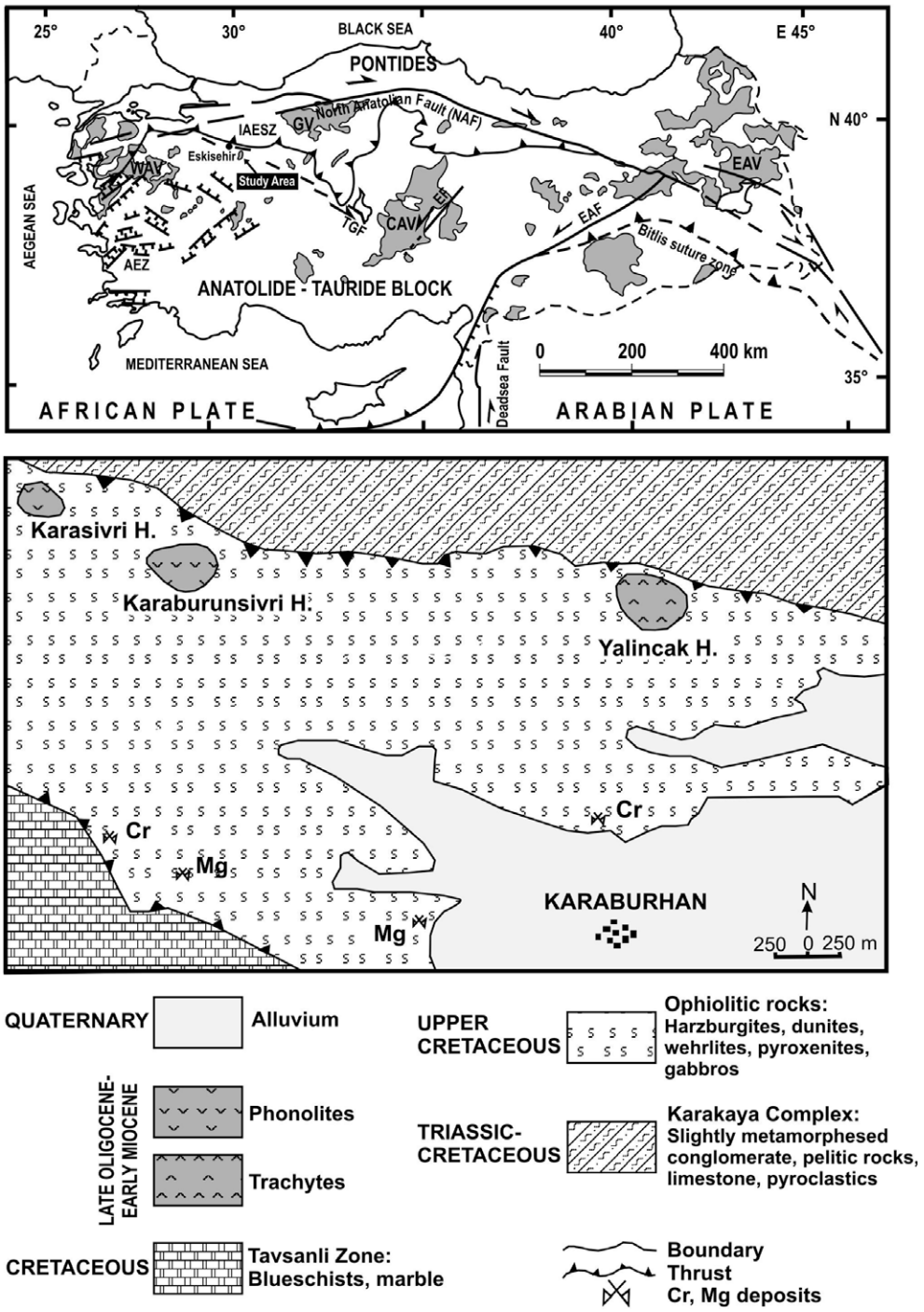

Fig. 1. Simplified map of Turkey showing general volcanological and main structural features (modified from Wilson et al., 1997; Genç and Yılmaz, 1997) and geological map of the investigated area (simplified from Gözler et al., 1996).

Considering the same-age volcanism in the western Anatolian volcanic province, Seyitoğlu and Scott (1992) showed that in Latest Oligocene–Early Miocene times, there was a change from N–S compression-related calc-alkaline magmatism to locally extension-related alkaline magmatism. Güleç (1991) considered that the sources of the western Anatolian rocks changed from shallow to deeper mantle magmas between the Early Miocene and the Quaternary. Aldanmaz et al. (2000) stressed that the Early to Middle Miocene calc-alkaline and shoshonitic rocks from western NW Anatolia were derived from lithospheric mantle sources with a subduction component whereas Late Miocene alkaline rocks were formed by partial melting of a garnet-bearing lherzolite source. Alıcı et al. (2002) suggested that the Kula lavas in western Anatolia are related to an extensional regime. The alkaline volcanic rocks were generated from mainly OIB-like asthenospheric magmas, with a limited contribution from lithosphere-derived melts. Keskin (2003) proposed that Middle Miocene–Pliocene volcanics of eastern Anatolia, ranging from rhyolitic to basaltic compositions, have been produced from asthenospheric mantle, including remnants of subducted material.

This article reports field observations and petrochemical studies of the phonolitic and trachytic volcanic cones around Karaburhan

(Sivrihisar–Eskisehir) in northwestern Anatolia. The objectives of this study were to date this volcanism using the $^{40}Ar/^{39}Ar$ method; to examine its petrogenesis by determining its chemical characteristics and Sr, Nd, and Pb isotopic compositions; and to discuss its role in the geodynamic evolution of the region.

2. Geological setting

Near Karaburhan, 20 km northwest of Sivrihisar (Eskisehir, Turkey), the Karasivri Hill and Karaburunsivri Hill phonolitic domes, together with the Yalincak Hill trachytic dome, cut through ophiolite nappe and are distributed parallel and close to the overthrust line (Fig. 1). The Upper Cretaceous SSZ-type ophiolites, remnants of the Izmir–Ankara–Erzincan ocean, representing the northern branch of the Neo-Tethyan Ocean between the Pontides and the Anatolide–Tauride Platform, consist of ultramafic–mafic rocks, such as harzburgites, dunites, wehrlites, pyroxenites, and gabbros (Sarifakioglu et al., 2006).

North of the ophiolite nappe, the Karakaya Complex of the Sakarya Continent (Pontides) comprises slightly metamorphosed conglomerates, sandstone, mudstone, spilitic pillow lavas, pyroclastics, and limestone blocks containing Permian–Carboniferous fossils (Bingöl et al., 1973; Bingöl, 1976; Okay et al., 1990). Hydrothermal mineralization veins consisting of Th- and rare earth elements (REEs) Ce, La, Y)-bearing fluorite–barite–bastnaesite are observed within the volcano-sedimentary rocks of the Karakaya Complex (Hatzle, 1992; Özgenç, 1993). South of the ophiolite nappe, the Tavsanli zone of the Anatolide–Tauride platform contains blueschist and marble (Okay, 1984; Okay and Tüysüz, 1999; Göncüoğlu et al., 2000).

In northwest Anatolia, a continent–continent collision occurred in the Upper Cretaceous–Early Eocene interval, when the northern Neo-Tethyan Ocean/Izmir–Ankara–Erzincan Ocean, between the Sakarya Continent in the north and the Anatolide–Tauride platform in the south, narrowed and finally disappeared (Yılmaz, 1990; Monod et al., 1991; Okay et al., 2001). The consequence of the N–S compressional regime that followed this collision was lithospheric thickening, with the crust reaching a thickness of 50 km (McKenzie, 1978; Le Pichon and Angelier, 1979; Şengör et al., 1984). The post-Middle Eocene N–S extension in response to this compressional regime resulted in the development of E–W trending faults, very much like the Aegean graben system. Linked to this tectonic regime, the local strike-slip faults formed in northwestern Anatolia. The Late Oligocene–Early Miocene phonolite and trachyte domes cross-cutting the ophiolite slab point to these faults parallel to the overthrust line in the studied area (Ozen and Sarifakioglu, 2003). This scenario indicates that the extensional regime reactivated the overthrust line in the form of local strike-slip faults, providing channels for the ascent of magma.

3. Analytical methods

The chemical composition of the phenocrystals and microphenocrystals of alkali feldspar, clinopyroxene, amphibole, hauyne, and analcime from the phonolites was determined by microprobe analysis. Mineralogical analyses were carried out on the phonolites using a Cameca SX-50-type electron microscope at the Department of Petrology at Pierre and Marie Curie University. The operating conditions were 15 kV accelerating voltage, 10–12 nA current, and 10 s counting time per element.

The formation age of the alkaline volcanics was determined using ^{40}Ar–^{39}Ar dating in the Department of Geological Sciences, Michigan University, using the laser step-heating method. Four sanidine macrocrystals were separated from two phonolite samples (P1 and P2) from Karaburunsivri Hill and irradiated for 4 h in location 5C in the McMaster Nuclear Reactor. Fish Canyon Tuff biotite split-3 (FCT-3) was used as a neutron-fluence monitor and has an Ar age of 27.99 ± 0.04 Ma relative to 520.4 Ma for the McClure Mountain hornblende standard (MMhb-1; Samson and Alexander, 1987; Hall and Farrell, 1995). This age is similar to the 27.95 ± 0.09 Ma age reported by Renne et al. (1998). The samples were incrementally heated with a Coherent Innova 5 W continuous argon-ion laser until complete fusion was achieved. Fusion system blanks were run after every five steps of the analysis, and the blank levels from argon masses 36–40 ($\sim 3 \times 10^{-18}$, $\sim 3 \times 10^{-18}$, $\sim 2 \times 10^{-18}$, $\sim 4 \times 10^{-18}$, and 3×10^{-16} mol, respectively) were subtracted from the sample analyses. Corrections were also made for the decay of ^{37}Ar and ^{39}Ar and for interfering nucleogenic reactions, as measured by K_2SO_4, KCl, and CaF. Before irradiation, the alteration surfaces of the sanidine crystals were cleaned by washing with acid and using an ultrasonic method.

The Sr, Nd, and Pb isotopic compositions of the alkaline volcanics have been determined at the ACT Analytical Laboratories Ltd., Canada. The Sr isotope analysis was performed with a Triton multicollector mass spectrometer in static mode. During the period of the work, the weighted average of 15 SRM-987 Sr standard runs yielded 0.710258 ± 11 (2s) for $^{87}Sr/^{86}Sr$. Sm and Nd were separated by extraction chromatography on hexyl di-ethyl hydrogen phosphate–covered Teflon® powder. The analysis was performed on a Triton multicollector mass spectrometer in static mode. The $^{143}Nd/^{144}Nd$ ratios are relative to the value of 0.511860 for the La Jolla standard. Pb was separated using an ion-exchange technique with BioRad 1 × 8 resin. Pb isotope compositions were analyzed on a Finnigan MAT-261 multicollector mass spectrometer. The measured Pb isotope ratios were corrected for the mass fractionation calculated from replicate measurements of Pb isotope compositions in the National Bureau of Standards SRM-982 standards. The external reproducibility of the Pb isotope ratios ($^{206}Pb/^{204}Pb$ = 0.1%; $^{207}Pb/^{204}Pb$ = 0.1%; $^{208}Pb/^{204}Pb$ = 0.2%) at the 2σ level was demonstrated with multiple analyses of standard BCR-1.

A total of 17 samples, 11 from phonolites and 6 from trachytes, were analyzed for major and trace (including rare earth) elements at the ACME and ACT Analytical Laboratories Ltd., Canada. The total abundances of the major oxides and several minor elements on a 0.2-g sample fused using lithium metaborate/tetraborate flux were analyzed by inductively coupled plasma (ICP) emission spectrometry. Loss on ignition (LOI) was calculated as the weight difference after ignition at 1000 °C. REEs were determined by ICP mass spectrometry following lithium metaborate/tetraborate fusion and nitric acid digestion of a 0.2-g sample.

4. Obtained results

4.1. Petrography and mineral chemistry

In the studied area, the Late Oligocene–Early Miocene phonolitic cones near Karasivri Hill and Karaburunsivri Hill form prominent twin peaks, cross-cutting the ultramafic tectonites (harzburgites) of the ophiolite slab. In the field, the partly altered light pinkish-grey phonolites can be observed as medium- to fine-grained rocks with aligned feldspar phenocrystals defining a fluidal texture. The trachytes observed at Yalincak Hill are light-cream-colored rocks with fine-grained feldspar crystals generally displaying a discernible orientation.

Under the microscope, the phonolites show hyalo-microlitic porphyritic and fluidal texture (Fig. 2a). The groundmass is composed of microcrystalline sanidine, clinopyroxene (aegirine,

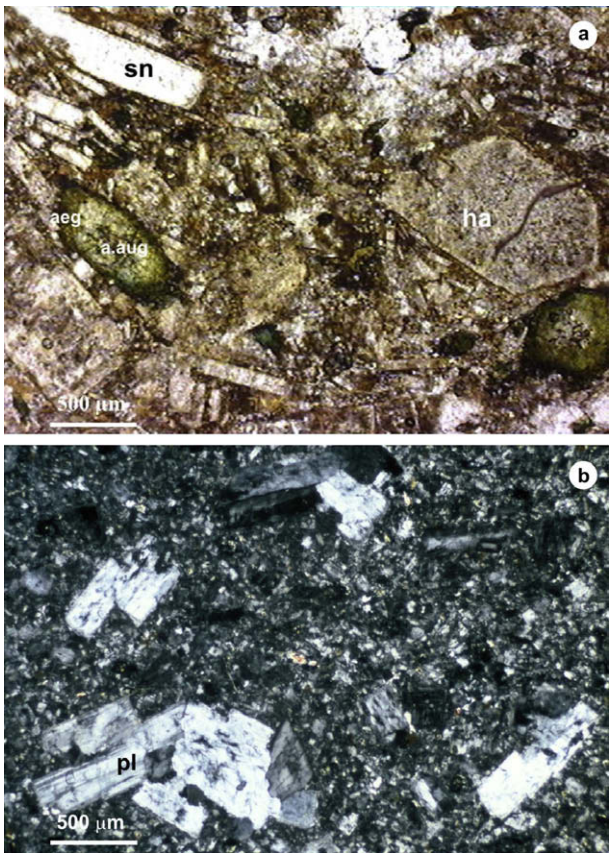

Fig. 2. (a) The photomicrograph with plane-polarized light from the phonolites (sn: sanidine; ha: hauyne; aeg: aegirine; a.aug: aegirine–augite); (b) the twinned plagioglase (pl) crystals in the trachytic texture in cross-polarized light.

aegirine–augite), feldspathoid (nepheline, hauyne), interstitial analcime, and volcanic glass. The phenocrystals and microlites of the alkali feldspar constitute about 65% of the rocks and are mainly sanidine ($Ab_{51-59}Or_{41-49}$) (Fig. 3). However, a few microlites of alkali feldspar show an anorthoclase composition ($Ab_{64-66}Or_{34-35}$) (Table 1). Euhedral or subhedral sanidine crystals may display carlsbad twinning, sometimes reaching 4 mm in length, and are partly argillized. The sanidine phenocrystals occasionally contain tiny aegirine–augite inclusions. Plagioclase (albite) is very rare. Both large and tiny feldspathoid crystals, which constitute about 25% of the mode, are hexagonal or rectangular in shape. Their phenocrystals are mostly altered to clay minerals, sericite, zeolite, and carbonate minerals. Microprobe analyses of the polygonal phenocrystals of the feldspathoid minerals show that they are mostly hauyne, with some nosean (Table 2). Nepheline and analcime microcrystals are also confined to the groundmass. The thin prismatic and sometimes needle-like aegirine–augites, which constitute about 10% of the rock, are generally green. The clinopyroxene phenocrystals commonly display compositional zoning, with dark green pleochroic aegirine rims ($Na_{0.82-0.96}Fe^{+3}{}_{0.68-0.83}$) and green–yellowish green pleochroic aegirine–augite cores, containing Ca and Mg, as well as Na and Fe (Table 3). The clinopyroxene microlites are generally aegirine–augite. Some aegirine–augite crystals have also been transformed to Na-, Ca-, and Mg-rich amphibole (hastingsite) (Table 4). Apatite and opaque minerals (Fe–Ti oxide) occur sporadically as accessory minerals. Apatite inclusions are common in altered hauyne crystals.

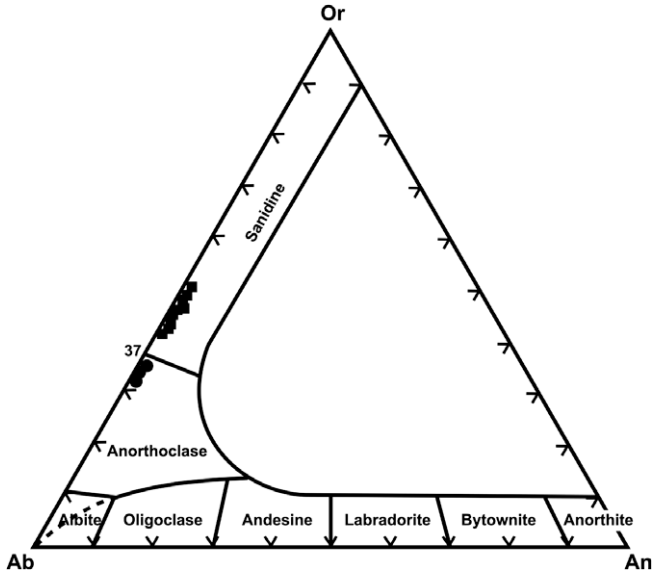

Fig. 3. Composition of alkali feldspars from the phonolites (■: sanidine; ●: anorthoclase).

The trachytes mainly consist of fine-grained feldspar crystals (Fig. 2b). Sanidine forms about 70% of the feldspars and defines a trachytic texture. The groundmass is mainly made up of sanidine microlites, with subordinate clinopyroxene and quartz. Plagioclase crystals (albite, oligoclase), which make up 15–20% of the feldspars, are aligned parallel to the fluidal texture and are partially altered to calcite and clay minerals. The euhedral to subhedral microphenocrystalline and microcrystalline augite crystals, which make up 7% of the rock, are partially altered to calcite, chlorite, or iron oxide minerals. Apatite crystals are accessory minerals but observed less than in the phonolites.

4.2. Ar–Ar geochronology and radiogenic isotopes

Four separate sanidine crystals were extracted from the phonolites. Based on isochron diagrams obtained for the single sanidine crystals taken from the phonolites, their ages are Late Oligocene–Early Miocene, ranging between 23.83 ± 1.2 Ma and 25.75 ± 0.3 Ma (Table 5). The detail data obtained from Ar–Ar age method are shown in Appendix A. The difference of 2 Ma in the ages of the four sanidine crystals belonging to P1 and P2 rock samples can be attributed to reset ages resulting from radiogenic Ar loss. The plateau ages are presented in Fig. 4. Özgenç (1993) previously reported K–Ar ages of 23.3 ± 3.2 and 26.2 ± 2.9 Ma for these alkaline volcanics. The small phonolitic and trachytic intrusions are close to each other and on the same line and also have similar chemical compositions. Therefore, they are thought to have formed at the same geological time (Late Oligocene–Early Miocene).

The Sr, Nd, and Pb isotopic compositions are given for five samples in Table 6. The $^{87}Sr/^{86}Sr$ and $^{143}Nd/^{144}Nd$ isotopic compositions of the phonolites range from 0.706358 to 0.706466 and from 0.512569 to 0.512646, respectively. The $^{87}Sr/^{86}Sr$ and $^{143}Nd/^{144}Nd$ values for the trachyte samples are 0.706553 to 0.708052 and 0.512546 to 0.512549, respectively. They were compared with extension-related volcanic rocks from western Turkey. Aldanmaz et al. (2000) have proposed that the Late Miocene alkaline rocks of Ezine–Gulpinar–Ayvacik (EGA) volcanics show OIB-type characteristics with low $^{87}Sr/^{86}Sr$ (0.70311–0.70325) and high $^{143}Nd/^{144}Nd$ (0.51293–0.51298), but Early–Middle Miocene Dikili–Ayvalik–Bergama (DAB) volcanics have characteristics indicating a mantle lithospheric source region carrying a subduction component with high $^{87}Sr/^{86}Sr$ (0.70757–0.70868) and low $^{143}Nd/^{144}Nd$ (0.51232–0.51246). The Kula volcanics are suggested

Table 1
Microprobe chemical analyses of alkali feldspar, crystals from the phonolites.

Sample no.	F3	F3	F3	F3	F3	F3	F2	F2	F2	F2	F2	F3	F3	F3	F3
Mineral	Microlites of sanidine				Microlites of anorthoclase			Cores of alkaline-feldspar				Rims of alkali-feldspars			
Analysis no.	2	11	12	13	14	15	23	19	20	21	22	3	6	7	10
SiO_2	65.94	65.61	65.53	65.41	66.08	65.56	63.65	66.63	66.06	66.54	65.87	65.87	65.52	65.24	65.62
TiO_2	0.00	0.00	0.00	0.00	0.00	0.00	0.00	0.00	0.00	0.00	0.00	0.00	0.00	0.00	0.00
Al_2O_3	19.09	18.92	18.84	18.88	19.15	19.12	20.12	19.35	19.16	19.19	19.03	18.81	19.17	19.03	19.04
Fe_2O_3	0.33	0.35	0.35	0.51	0.43	0.32	0.25	0.39	0.17	0.33	0.42	0.31	0.29	0.34	0.31
MnO	0.00	0.00	0.00	0.00	0.00	0.00	0.00	0.00	0.00	0.00	0.00	0.00	0.00	0.00	0.00
MgO	0.01	0.03	0.00	0.00	0.00	0.00	0.00	−0.01	−0.01	−0.02	0.00	0.00	0.00	0.00	0.00
CaO	0.04	0.02	0.08	0.01	0.09	0.15	0.20	0.06	0.10	0.08	0.06	0.04	0.07	0.07	0.02
Na_2O	6.28	6.27	5.65	5.94	7.14	7.11	7.20	6.01	6.19	6.24	6.53	6.30	5.67	5.55	5.84
K_2O	6.82	6.98	7.82	7.63	5.59	5.56	5.90	7.35	7.15	7.14	6.69	6.72	7.95	8.13	7.89
Total	98.48	98.14	98.25	98.38	98.46	97.79	97.30	99.76	98.81	99.49	98.57	98.03	98.64	98.32	98.69
Formula on the basis of eight oxygens															
	32	32	32	32	32	32	32	32	32	32	32	32	32	32	32
Si	11.955	11.953	11.96	11.932	11.941	11.927	11.698	11.946	11.954	11.959	11.941	11.991	11.919	11.919	11.933
Ti	0.000	0.000	0.000	0.000	0.000	0.000	0.000	0.000	0.000	0.000	0.000	0.000	0.000	0.000	0.000
Al	4.080	4.063	4.052	4.06	4.078	4.1	4.358	4.09	4.088	4.065	4.066	4.036	4.111	4.099	4.082
Fe3+	0.045	0.048	0.049	0.071	0.058	0.044	0.035	0.052	0.023	0.045	0.057	0.042	0.039	0.046	0.042
Mn	0.000	0.000	0.000	0.000	0.000	0.000	0.000	0.000	0.000	0.000	0.000	0.000	0.000	0.000	0.000
Mg	0.002	0.007	0.001	0.000	0.000	0.000	0.000	-0.001	-0.003	-0.004	0.001	0.001	0.000	0.000	0.000
Ca	0.008	0.004	0.016	0.003	0.018	0.03	0.039	0.012	0.018	0.015	0.012	0.008	0.014	0.013	0.003
Na	2.208	2.214	2.001	2.103	2.503	2.508	2.566	2.089	2.172	2.174	2.294	2.225	1.999	1.965	2.058
K	1.577	1.621	1.821	1.775	1.29	1.29	1.383	1.682	1.652	1.637	1.548	1.56	1.844	1.894	1.832
Total	19.875	19.91	19.9	19.942	19.887	19.899	20.08	19.869	19.903	19.891	19.919	19.863	19.927	19.937	19.95
Ab	58.2	57.7	52.1	54.2	65.7	65.5	64.3	55.2	56.5	56.8	59.5	58.7	51.8	50.7	52.9
Or	41.6	42.2	47.5	45.7	33.8	33.7	34.7	44.5	43	42.8	40.2	41.1	47.8	48.9	47
An	0.2	0.1	0.4	0.1	0.5	0.8	1	0.3	0.5	0.4	0.3	0.2	0.4	0.3	0.1

Table 2
Chemical compositions for feldspathoid crystals.

Sample no.	F3	F3	F3	F2	F2	F2	F2
Mineral	Hauyne				Analcime		
Analysis no.	16	17	18	27	24	25	28
SiO_2	40.94	43.16	41.54	38.74	54.03	53.33	54.37
TiO_2	0.00	0.01	0.00	−0.01	0.00	0.00	0.00
Al_2O_3	28.31	29.21	28.34	29.30	22.47	23.80	22.84
FeO	1.47	1.12	0.04	0.04	0.33	1.50	0.04
MnO	0.00	0.00	0.00	0.00	0.00	0.00	0.00
MgO	0.04	0.03	0.05	0.01	−0.01	−0.01	0.00
CaO	9.29	9.37	9.72	12.15	0.06	0.13	0.03
Na_2O	5.33	2.12	5.47	3.48	12.34	10.85	12.76
K_2O	0.04	0.03	0.02	0.01	0.15	0.64	0.15
Total	85.43	85.04	85.19	83.94	89.39	90.26	90.18

to have been predominantly generated from OIB-like asthenospheric mantle sources with $^{87}Sr/^{86}Sr$ (0.703029–0.703490) and $^{143}Nd/^{144}Nd$ (0.512773–0.512941) (Alıcı et al., 2002). However, the alkaline Oglakci trachytes with $^{87}Sr/^{86}Sr$ (0.7054–0.7056) and $^{143}Nd/^{144}Nd$ (0.512713–0.512674) near the studied area are considered to have originated from within-plate volcanism (Temel, 2001). The Late Miocene alkaline lavas of the EGA and Kula volcanics with OIB-like compositions plot within the mantle array, but the Late Oligocene–Early Miocene alkaline volcanics, the Early–Middle Miocene volcanic rocks of DAB, and Oglakci trachytes occur apart from the mantle array, indicating subduction enrichment (Fig. 5).

The plotting of the alkaline Sivrihisar volcanics is next to oceanic sediments or enriched mantle-II (EMII) subfields in Fig. 6a and b. EMII is characterized by high ($^{87}Sr/^{86}Sr$), low ($^{143}Nd/^{144}Nd$), and high- to intermediate $^{207}Pb/^{204}Pb$, $^{208}Pb/^{204}Pb$, and $^{206}Pb/^{204}Pb$ (Zindler and Hart, 1986). Such Pb isotopic compositions imply a similarity of the geochemical features of continental crust and continent-derived sediments in genesis. The alkaline volcanic rocks have $^{207}Pb/^{204}Pb$ (~15.74), $^{208}Pb/^{204}Pb$ (~39.25), and $^{206}Pb/^{204}Pb$ (~18.94) values. The alkaline lavas generated from a lithospheric mantle enriched by subduction-related processes have been affected by continent-derived sediments and/or the subduction of terrigenous flysch passing through thickened crust.

4.3. Geochemistry

The silica-undersaturated phonolites contain about 56% SiO_2; the trachytes contain approximately 64% SiO_2 (Table 7). The LOI is higher in the phonolites than in the trachytes, and field and petrographic observations suggest that the phonolites have undergone hydrothermal alteration. We suggest that this alteration also caused mobility and expulsion of some large-ion lithophile elements (LILEs) (Hart et al., 1974; Humphris and Thompson, 1978).

The total alkalis vs. silica (TAS) diagram shows that the Late Oligocene–Early Miocene volcanics fall in the field of phonolites and trachytes (Fig. 7a). They also plot to the phonolite and trachyte field in the Zr/Ti vs Nb/Y diagram (Fig. 7b). The phonolites have high Ba (859–1446 ppm), Sr (860–1196 ppm), Rb (139–174 ppm), and Th (258–308 ppm) contents, whereas the trachytes tend to contain higher Ba (1349–3984 ppm) and Sr (1859–2571 ppm) but lower Rb (76–123 ppm) and Th (40–46 ppm). The Nb values for the phonolites (224.1–392 ppm) are higher than those of the trachytes (27.8–57.5 ppm). The Ta values are less than Nb values in the alkaline rocks, at 9.75–7.7 ppm in the phonolites and 2.02–1.7 ppm in the trachytes. High Pb contents (175–293 ppm) are observed in the phonolites, but lower Pb contents (18–49 ppm) are found in the trachytes. The trace element characteristics of the alkaline lavas generally resemble those of lavas derived from lithospheric mantle enriched by subduction-related processes and/or contaminated by crustal materials.

Table 3
Microprobe data of clinopyroxene crystals belonging to the phonolites.

Sample no.	F3	F3	F3	F3	F3	F3	F2	F2	F2	F2	F2	F2	F2	F2	F2	F2
Mineral	Cpx	Cpx	Cpx	Cpx	Cpx	Cpx	Cpx	Cpx	Cpx	Cpx	Cpx	Cpx	Cpx	Cpx	Cpx	Cpx
Analysis no.	1	10	12	11	14	15	111	112	116	117	118	121	122	123	124	125
	The rims of clinopyroxenes				The microlites				The rims of microphenocrystals				The cores of microphenocrystals			
SiO_2	50.34	50.28	50.31	50.18	51.10	51.65	52.36	51.75	52.50	52.54	52.51	52.10	51.62	50.76	50.78	49.10
TiO_2	0.45	0.26	0.35	0.33	0.41	0.39	0.40	0.24	2.71	2.29	1.52	1.15	0.47	0.32	0.24	0.13
Al_2O_3	2.02	1.56	1.77	1.77	1.05	0.68	0.53	1.18	0.76	0.72	0.78	0.63	0.71	0.85	2.20	0.93
Cr_2O_3	0.11	0.05	0.06	0.00	0.00	0.00	0.00	0.01	0.00	0.10	0.00	0.08	0.01	0.00	0.00	0.04
FeO	18.02	17.74	18.01	17.76	23.56	26.98	26.57	20.15	26.44	27.09	27.83	26.56	26.54	23.52	17.90	17.54
MnO	1.18	1.23	1.03	1.30	1.11	0.53	0.54	1.26	0.43	0.33	0.27	0.51	0.59	0.97	0.90	1.10
MgO	5.47	6.04	5.63	5.40	2.63	0.98	1.36	4.34	0.44	0.42	0.44	0.70	1.02	2.31	4.77	3.58
CaO	17.92	18.67	18.12	18.02	12.55	6.59	7.27	12.97	1.35	1.60	1.60	4.34	7.26	12.51	13.96	19.77
Na_2O	3.45	3.34	3.22	3.23	6.33	9.77	9.52	5.94	13.01	13.00	12.78	10.89	9.43	6.35	6.37	5.01
K_2O	0.03	0.00	0.04	0.00	0.00	0.01	0.00	0.05	0.01	0.03	0.00	0.02	0.00	0.00	0.14	0.00
	99.06	99.25	98.58	98.01	98.79	97.58	98.68	97.88	97.70	98.13	98.05	96.98	97.72	97.67	97.35	99.82
Formula calculated based on six oxygens																
Si	1.949	1.939	1.959	1.966	1.986	2.001	2.009	2.006	1.995	1.988	1.996	2.019	2.003	1.998	1.955	1.922
Al	0.092	0.071	0.081	0.082	0.048	0.031	0.024	0.054	0.034	0.032	0.035	0.029	0.033	0.039	0.100	0.043
Cr	0.003	0.001	0.002	0.000	0.000	0.000	0.000	0.000	0.000	0.003	0.000	0.002	0.000	0.000	0.000	0.001
Ti	0.013	0.008	0.010	0.010	0.012	0.011	0.012	0.007	0.077	0.065	0.043	0.034	0.014	0.009	0.007	0.004
Fe^{2+}	0.583	0.572	0.586	0.582	0.766	0.874	0.853	0.653	0.840	0.857	0.885	0.861	0.861	0.774	0.577	0.574
Mn	0.039	0.040	0.034	0.043	0.037	0.017	0.018	0.041	0.014	0.011	0.009	0.017	0.020	0.032	0.030	0.036
Mg	0.316	0.347	0.327	0.315	0.152	0.056	0.078	0.251	0.025	0.024	0.025	0.041	0.059	0.136	0.274	0.209
Ca	0.744	0.772	0.756	0.757	0.522	0.274	0.299	0.539	0.055	0.065	0.065	0.180	0.302	0.527	0.576	0.829
Na	0.259	0.249	0.243	0.245	0.477	0.734	0.708	0.446	0.959	0.954	0.942	0.818	0.710	0.484	0.476	0.381
K	0.001	0.000	0.002	0.000	0.000	0.000	0.000	0.002	0.000	0.001	0.000	0.001	0.000	0.000	0.007	0.000
Total	4.000	4.000	4.000	4.000	4.000	4.000	4.000	4.000	4.000	4.000	4.000	4.000	4.000	4.000	4.000	4.000
Fe^{3+}	0.240	0.283	0.224	0.212	0.433	0.678	0.643	0.368	0.780	0.814	0.827	0.683	0.645	0.431	0.459	0.484
Fe^{2+}	0.343	0.289	0.362	0.37	0.333	0.197	0.210	0.285	0.061	0.043	0.058	0.177	0.217	0.343	0.118	0.091

Table 4
Chemical compositions for amphibole crystals from the alkaline volcanics.

Sample no.	F3	F3	F3
Mineral	Hastingsite		
Analysis no.	4	5	9
SiO_2	40.12	41.87	40.63
TiO_2	1.95	1.81	1.98
Al_2O_3	11.68	10.69	11.63
FeO	18.49	14.88	16.24
MnO	0.60	0.42	0.35
MgO	8.92	11.49	10.30
CaO	11.05	11.28	11.13
Na_2O	3.07	3.21	3.09
K_2O	1.60	1.43	1.44
Cl	0.01	0.00	0.02
F	0.57	1.55	1.43
	98.07	98.62	98.25
Formula calculated based on 23 oxygens			
	23.00	23.00	23.00
Si	6.196	6.361	6.236
Al	2.126	1.913	2.103
Ti	0.226	0.206	0.229
Fe	2.388	1.890	2.085
Mn	2.054	2.603	2.357
Mg	2.054	2.603	2.357
Ca	1.828	1.837	1.830
Na	0.918	0.945	0.919
K	0.315	0.277	0.283
Total	18.106	18.636	18.397

Ratios of Nb/Y > 1.5 and Zr/Nb < 6 are typical features of alkaline lavas erupted in an extensional setting (Edwards et al., 1991). The alkaline volcanics in the studied area have high Nb/Y ratios (1.3–14.5) and low Zr/Nb ratios (2.10–5.88). High Ba/Ta (>450) and Ba/Nb (>28) ratios are characteristic features of subduction-related magmas (Fitton et al., 1998). The phonolites exhibit low Ba/Nb (3–5) and Ba/Ta (100–180) ratios, but the trachytes contain higher Ba/Nb (26–91) and Ba/Ta (748–2213) ratios. These variations imply that the trachytes exhibit more effects of subduction components from a lithospheric mantle source than the phonolites.

Chemical analyses of the alkaline lavas show enrichment in LILEs (Sr, K, Rb, Ba, Th) and some high-field-strength elements (HFSE: Nb, Ta, Zr, Hf) relative to the mid-oceanic-ridge basalts (MORBs), showing typical OIB-like geochemical characteristics (Fig. 8a). However, they are negative anomalies in Nb and Ta relative to Th and K, which is not consistent with the geochemical features of the OIBs (Sun and McDonough, 1989). This finding implies a lithospheric mantle source affected by subduction components. The P_2O_5 and TiO_2 depletion in the alkaline lavas are probably related to apatite and titanomagnetite fractionation, respectively. Samples SP-1 and SP-29 from the phonolites have slightly higher concentrations of LILEs (especially Th) and the light REEs (LREEs). This feature could be related to the hydrothermal mineralization of Th- and REE (Ce, La, Y)-bearing fluorite–barite–bastnaesite ore deposits about 5 km north of the alkaline domes (Hatzle, 1992; Özgenç, 1993).

Table 5
Ar-isotope results and isochron ages of sanidine crystals from the phonolites.

Sample no.	J	$^{40}Ar/^{39}Ar$	$^{40}Ar/^{36}Ar$	MSWD	n	All points time (Ma)	Total gas age (Ma)
s11aP1	$9.99 \times 10^{-4} \pm 1.69 \times 10^{-6}$	2.774 ± 0.369	270.7 ± 9.6	14.11	13	25.75 ± 0.33	24.58 ± 0.08
s11bP1	$9.99 \times 10^{-4} \pm 1.69 \times 10^{-6}$	2.414 ± 0.259	277.6 ± 17.4	6.82	10	25.19 ± 0.49	24.53 ± 0.11
s12aP2	$9.75 \times 10^{-4} \pm 2.29 \times 10^{-6}$	1.726 ± 0.234	252.5 ± 14.0	20.04	13	25.29 ± 0.37	24.20 ± 0.08
s12bP2	$9.75 \times 10^{-4} \pm 2.29 \times 10^{-6}$	2.783 ± 0.481	302.9 ± 25.5	14.81	11	23.83 ± 1.38	24.35 ± 0.12

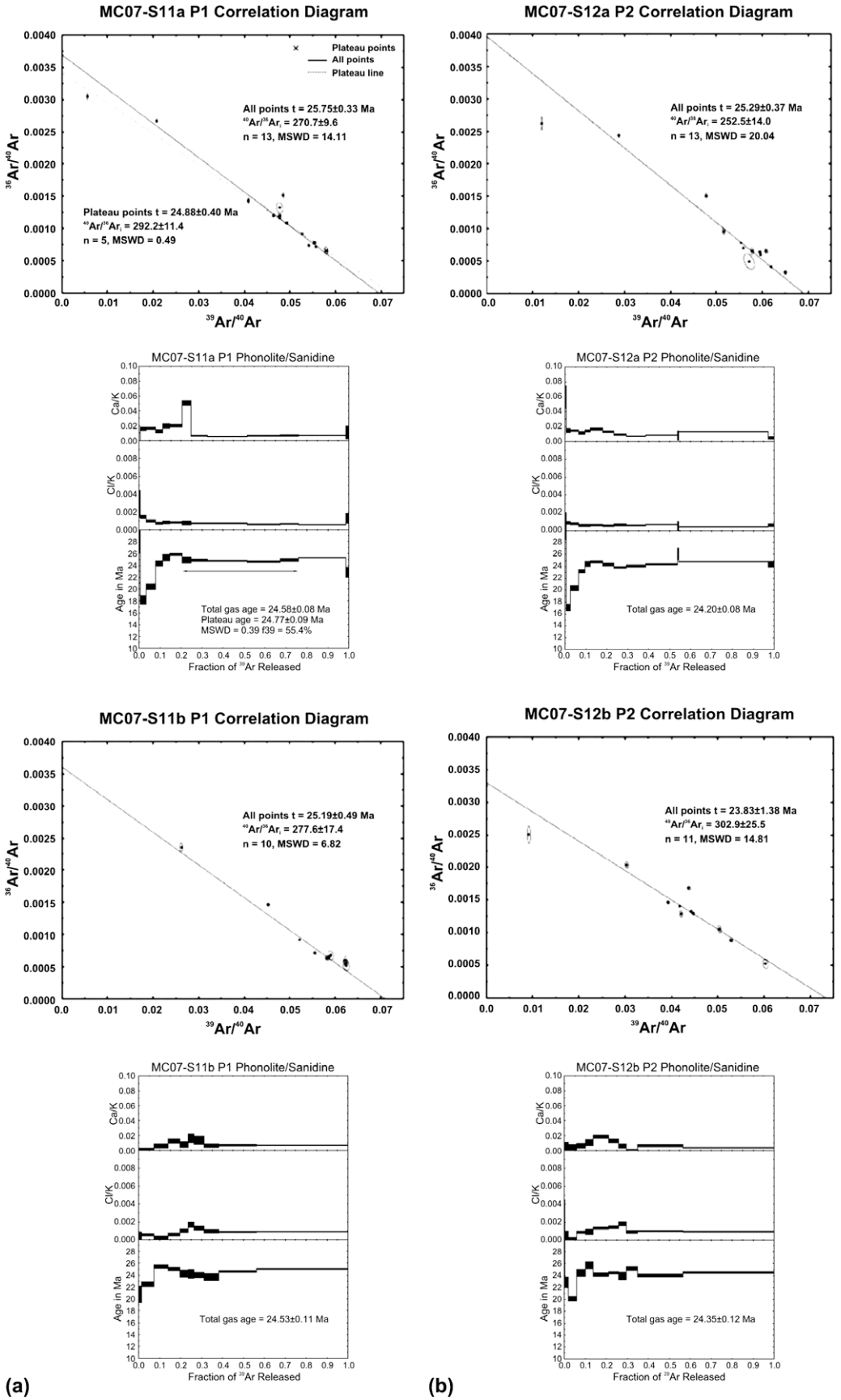

Fig. 4. Ar/Ar age results. $^{39}Ar/^{40}Ar$–$^{36}Ar/^{40}Ar$ isochrons and age spectra of sample P1 (a) and sample P2 (b), respectively.

Table 6
Sr, Nd and Pb isotope data for alkaline volcanic rocks from the Karaburhan area.

Sample no.	SP 28	SP 45	SP 46	ST 13	ST 27
Rock type	Phonolite	Phonolite	Phonolite	Trachyte	Trachyte
$^{206}Pb/^{204}Pb$	18.946	18.939	18.951	18.752	19.111
$^{207}Pb/^{204}Pb$	15.752	15.744	15.756	15.739	15.71
$^{208}Pb/^{204}Pb$	39.319	39.285	39.342	39.064	38.956
$^{87}Sr/^{86}Sr$	0.706358	0.706545	0.706466	0.706553	0.708052
± 2σm	0.000006	0.000006	0.000007	0.000006	0.000008
$^{143}Nd/^{144}Nd$	0.512569	0.512646	0.512576	0.512546	0.512549
±2σm	0.000002	0.000002	0.000002	0.000002	0.000002
eNd(0)	−1.3	0.2	−1.2	−1.8	−1.7
Rb (ppm)	168	149	151	105	123
Sr (ppm)	1196	860	873	2085	2099
Sm (ppm)	9.37	8.21	8.23	7.95	2.75
Nd (ppm)	60.7	52.5	53.1	55.3	12.5
$^{87}Rb/^{86}Sr$	0.406	0.501	0.500	0.146	0.170
$^{147}Sm/^{144}Nd$	0.0933	0.0945	0.0937	0.0869	0.1330
f (Sm/Nd)	−0.53	−0.52	−0.52	−0.56	−0.32
eNd (25 Ma)	−1.0	0.5	−0.9	−1.4	−1.5
ISr (25 Ma)	0.70621	0.70637	0.70629	0.70650	0.70799

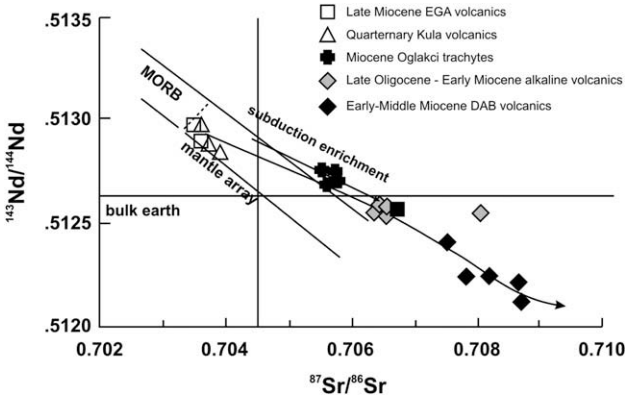

Fig. 5. $^{143}Nd/^{144}Nd$ vs. $^{87}Sr/^{86}Sr$ isotope diagram showing the representative the Late Oligocene–Early Miocene alkaline volcanics, Late Miocene EGA volcanics and Early–Middle Miocene DAB volcanics (Aldanmaz et al., 2000), Quaternary Kula volcanics (Alıcı et al., 2002) and Miocene Oglakci trachytes (Temel, 2001). MORB and OIB composition fields from Zindler and Hart (1986). The curve related subduction enrichment after DePaolo (1981).

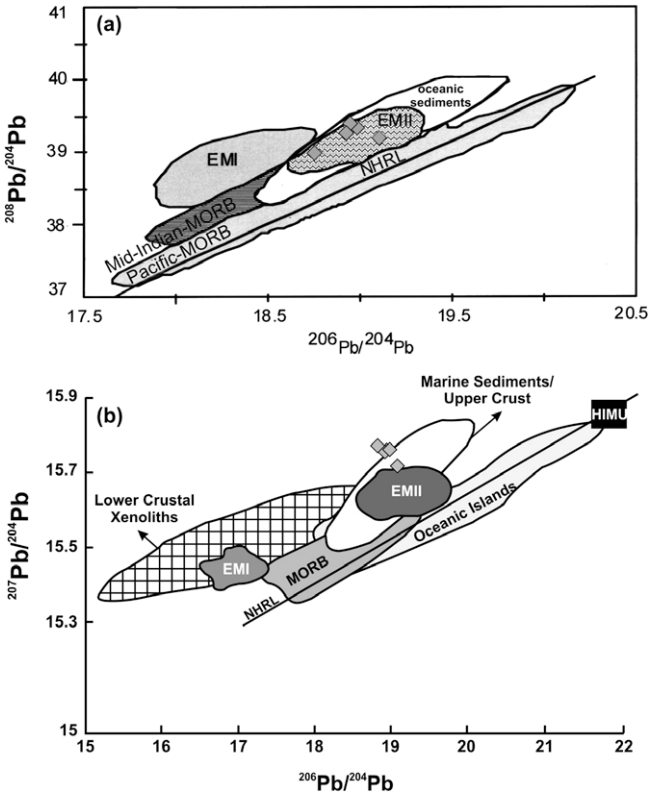

Fig. 6. $^{206}Pb/^{204}Pb$ vs. $^{208}Pb/^{204}Pb$ and $^{206}Pb/^{204}Pb$ vs. $^{207}Pb/^{204}Pb$ variation diagrams of the alkaline volcanics rocks. Composition fields for upper and lower crust, MORB (mid-ocean ridge basalts), HIMU (enriched mantle in U and Th relative to Pb), OIB (oceanic island basalts), EMI (enriched mantle I) and EMII (enriched mantle II) from Zindler and Hart (1986). Northern Hemisphere Reference Line indicated (NHRL).

All of the alkaline volcanics show enrichment in LREEs and a flat pattern from Dy towards Lu (Fig. 8b). However, the heavy REE (HREE) concentrations of the trachytes are less than those for the phonolites. This strong enrichment in LREEs relative to HREEs suggests a within-plate trend, showing that their eruption took place in an extensional setting.

Norman and Garcia (1999) stressed that magmas that have undergone crustal contamination have low Ce/Pb ratios (<2.5). Low Ce/Pb ratios (~1) and high Pb contents (175–293 ppm) are observed in the phonolites, and lower Pb contents (18–49 ppm) were found in the trachytes. Their Pb contents may have been caused by significant crustal contamination during their ascent along faults in the region.

5. Discussion

5.1. Petrogenetic modeling

5.1.1. Fractional crystallization and crustal contamination

Major and trace element contents reflect the significant role of fractional crystallization processes during the evolution of the alkaline volcanics. The high Na_2O, K_2O, and Al_2O_3 concentrations and consumption of CaO can be explained by the fractionation of sanidine crystals, feldspathoids (hauyne, nosean, nepheline) and clinopyroxenes (aegirine–augite) in the phonolites. The trachyte samples have higher SiO_2 and less Fe_2O_3, MgO, CaO, and Al_2O_3 contents, probably as a result of crystallization of plagioclase and clinopyroxene (augite) crystals. The depletion in P_2O_5 and TiO_2 is probably related to apatite and titanomagnetite fractionation, respectively.

According to trace element and isotopic compositions, the alkaline volcanics are rich in Ba (859–3984 ppm), Rb (76–174 ppm), and Sr (860–2571 ppm) and also have high $^{87}Sr/^{86}Sr$ (0.706358–0.708052), $^{207}Pb/^{204}Pb$ (15.710–15.756), and $^{208}Pb/^{204}Pb$ (38.956–39.342), and low $^{206}Pb/^{204}Pb$ (18.752–19.111), suggesting crustal contamination when they rise through the thick crust. These chemical characteristics suggest that they were derived from lithospheric mantle enriched by subducted terrigenous and carbonate sediments. The alkaline volcanics have low ε_{Nd} values. The initial ε_{Nd} values range from −1.5 to 0.5 while the recent ε_{Nd} values vary between −1.8 and 0.2 (Table 6). The values of ε_{Nd} and $^{87}Sr/^{86}Sr$ ratios indicate that assimilation and fractional crystallization played a major role during magmatic evolution of Oligo–Miocene alkaline rocks.

In theoretical assimilation and fractional crystallization (AFC) modeling (DePaolo, 1981), trace element contents and Sr isotope compositions were used. In the modeling, the '*r*' value was represented as the AFC numeric index. As shown in Fig. 9, the $^{87}Sr/^{86}Sr$ vs Rb/Sr diagram contains '*r*' curves, reflecting AFC

Table 7
Whole rock chemical analyses of phonolites and trachytes.

Lithology	Phonolites											Trachytes						
Sample no.	SP.28	SP.29	SP.30	SP.31	SP.45	SP.46	SP.1	SP.2	SP.3	SP.4	SP.5	ST.13	ST.27	ST.1	ST.2	ST.3	ST.4	ST.5
SiO_2	57.01	55.53	55.96	56.70	55.62	57.32	56.14	56.24	56.03	56.51	56.41	64.90	64.70	64.82	63.77	64.39	63.96	63.74
TiO_2	0.21	0.22	0.21	0.20	0.21	0.20	0.22	0.20	0.20	0.20	0.21	0.42	0.10	0.42	0.40	0.40	0.39	0.39
Al_2O_3	18.94	19.75	19.67	18.89	18.55	19.07	18.57	18.84	18.76	19.15	19.21	17.45	15.44	16.29	16.39	16.35	16.32	16.09
Fe_2O_3	2.72	2.88	2.75	2.56	2.61	2.59	2.88	2.65	2.58	2.67	2.68	2.13	2.48	2.23	2.40	2.30	2.27	2.27
MnO	0.170	0.170	0.153	0.152	0.151	0.149	0.15	0.14	0.14	0.15	0.14	0.020	0.13	0.05	0.06	0.05	0.03	0.05
MgO	0.72	0.63	0.77	0.69	0.32	0.32	0.65	0.32	0.77	0.42	0.41	0.50	0.34	0.58	0.55	0.54	0.54	0.66
CaO	2.12	2.37	2.08	2.00	3.35	2.18	2.15	2.09	2.08	2.07	2.07	1.39	3.02	1.40	2.02	2.02	2.15	2.25
Na_2O	**6.98**	**7.18**	**7.28**	**7.02**	**6.80**	**7.01**	**6.94**	**7.00**	**7.08**	**6.83**	**6.86**	**6.20**	**5.70**	**5.43**	**5.66**	**5.53**	**5.54**	**5.52**
K_2O	**5.46**	**5.68**	**5.82**	**5.21**	**5.08**	**5.37**	**5.44**	**5.55**	**5.28**	**5.09**	**5.14**	**4.88**	**3.88**	**4.84**	**4.22**	**4.29**	**4.16**	**4.18**
P_2O_5	0.04	0.04	0.03	0.04	0.05	0.04	0.02	0.02	<0.01	0.01	0.02	0.22	0.14	0.19	0.17	0.19	0.17	0.17
LOI	4.58	4.49	5.07	5.16	5.91	5.09	6.10	6.30	5.90	5.80	5.80	1.72	3.34	3.20	3.20	2.80	3.40	3.40
SUM	98.96	98.93	99.79	98.61	98.63	99.32	99.36	99.46	100.2	99.06	99.11	99.83	99.27	99.61	99.22	99.2	99.18	99.18
Ba	**953**	**979**	**963**	**890**	**918**	**979**	**859**	**948**	**1028**	**1402**	**1446**	**1510**	**1457**	**1349**	**3242**	**2856**	**3984**	**3984**
Ni	<20	<20	<20	<20	<20	<20	<20	<20	42	<20	<20	100	116	66	116	79	70	70
Sc	1	<1	1	1	1	1	11	10	1	1	1	3	4	3	3	3	3	3
Co	1	2	2	1	1	1	85	30	13	12	18	6	30	47	24	16	19	19
Cs	17.4	17.3	14.3	14.6	10.9	15.2	16.6	15.1	12.8	15.6	14.3	2.6	5.7	2.1	1.6	1	0.9	0.9
Ga	44	50	50	44	41	43	49	46	40	38	38	37	25	36	32	29	29	29
Hf	20.5	22.9	20.6	19.6	19.2	18.8	22.7	19.5	18.3	19.9	19.1	5.0	5.9	4.9	5.6	4.4	4.5	4.5
Nb	266	392	361	249	236	240	262.4	224.1	269.8	271.9	277.9	57.5	27.8	38.7	45.2	42.7	43.6	43.6
Rb	**168**	**174**	**172**	**152**	**149**	**151**	**159**	**141**	**146**	**142**	**139**	**105**	**123**	**98**	**81**	**76**	**77**	**77**
Sn	3	4	3	3	3	3	4	5	3	3	3	2	2	2	1	<1	1	1
Sr	**1196**	**1183**	**910**	**925**	**860**	**873**	**1125**	**899**	**883**	**939**	**960**	**2085**	**2099**	**1859**	**2123**	**2437**	**2571**	**2571**
Ta	9.21	9.75	8.97	8.59	8.61	8.43	8.4	7.7	7.9	7.8	8.1	2.02	1.9	1.8	1.9	1.7	1.8	1.8
Th	**305**	**286**	**258**	**278**	**277**	**270**	**308**	**275**	**264**	**285**	**277**	**44**	**40**	**43**	**43**	**43**	**46**	**46**
U	72	79.3	70.5	64.4	61.1	61.8	74	59.8	66.8	63	60.3	8.5	8.6	8.5	9.6	8.7	8.9	8.9
V	42	40	38	37	38	49	39	36	35	35	35	37	34	34	42	29	34	34
Zr	**1340**	**1370**	**1280**	**1290**	**1250**	**1230**	**1318**	**1141**	**1189**	**1181**	**1205**	**243**	**57**	**212**	**266**	**197**	**208**	**208**
Y	25.9	27.7	24.9	23.6	23.8	23.2	26	22	23	23	24	11.3	22.4	10	12	16	15	15
La	119	123	100	102	99.4	98.8	125.4	97.3	97.1	98.9	99.1	98.9	15.3	100.7	95.9	112.3	99.4	99.4
Ce	213	219	182	186	182	181	210.8	168.1	176.5	179	180.7	153	30.1	148.2	158.8	152.6	151.6	151.6
Pr	21.8	21.0	17.6	19.2	18.6	18.6	20.95	16.73	17.08	17.73	17.64	16.2	3.13	16.47	16	18.22	16.65	16.65
Nd	60.7	65.0	56.3	54.5	52.5	53.1	66.7	54	55.1	57.2	58.7	55.3	12.5	57.5	56.7	66	60.4	60.4
Sm	9.37	10.5	9.20	8.34	8.21	8.23	9.8	8	8.2	8.4	8.4	7.95	2.75	7.4	7	8.2	7.5	7.5
Eu	2.40	2.57	2.19	2.22	2.14	2.13	2.54	2.07	2.03	2.11	2.23	2.04	0.54	2	1.97	2.28	1.9	1.9
Gd	5.82	6.91	5.65	5.32	5.36	5.18	5.45	4.62	5.36	4.89	5.34	4.83	2.67	3.33	4.24	4.95	4.69	4.69
Tb	0.85	0.95	0.79	0.77	0.78	0.72	0.86	0.72	0.75	0.75	0.73	0.54	0.50	0.43	0.48	0.54	0.5	0.5
Dy	4.42	4.67	4.04	4.03	4.01	3.87	4.33	3.66	3.79	3.9	3.84	2.25	3.01	2.06	2.02	2.66	2.32	2.32
Ho	0.87	0.86	0.76	0.76	0.77	0.74	0.73	0.66	0.68	0.69	0.7	0.37	0.64	0.29	0.33	0.39	0.37	0.37
Er	2.51	2.50	2.23	2.27	2.29	2.21	2.35	1.85	1.96	2.04	2.1	0.96	2.00	0.72	0.87	1.17	1.06	1.06
Tm	0.41	0.41	0.37	0.38	0.37	0.36	0.35	0.30	0.36	0.32	0.33	0.135	0.33	0.11	0.14	0.17	0.17	0.17
Yb	2.74	2.77	2.49	2.55	2.56	2.38	2.88	2.33	2.32	2.16	2.46	0.81	2.27	0.76	0.78	0.98	0.94	0.94
Lu	0.392	0.420	0.368	0.364	0.380	0.375	0.41	0.36	0.39	0.38	0.39	0.104	0.35	0.11	0.12	0.15	0.14	0.14
Pb	**195**	**293**	**263**	**217**	**216**	**213**	**221**	**193**	**175**	**200**	**190**	**49**	**29**	**18**	**31**	**27**	**31**	**33**

effects in the volcanic rocks from northwestern Central Anatolia and western Anatolia. The studied alkaline rocks of the Sivrihisar (Eskisehir) region are observed at $r = 0.2–0.3$, and the Early–Middle Miocene–aged volcanic rocks of western Anatolia are at $r = 0.3$ (Aldanmaz et al., 2000). The characteristic geochemical signatures of the alkaline volcanics suggest that assimilation, fractional crystallization, and crustal contamination processes were responsible for the evolution of these alkaline magmas.

5.1.2. The source characteristics of the alkaline magmas

The trace element data and isotopic compositions suggest that the alkaline lavas were derived from a lithospheric mantle that had been modified by fluid-melting processes linked to previous subducted slab. The mantle-derived magmas have undergone crustal contamination, having been erupted in an extensional setting. The collision volcanism in northwestern Anatolia has been closely linked to collision with the Pontides and Anatolide–Tauride Platform as a result of the closure of the northern branch of the Neo-Tethyan Ocean along the Izmir–Ankara–Erzincan Suture Zone (IAESZ). Harris et al. (1994) proposed that the timing of the collision was Late Paleocene–Early Eocene, using obduction of the ophiolite slabs known as the remnants of this ocean exposed along the suture zone. This collision caused the small pull-apart basins generated by the extensional tectonic regime in western and northwestern Anatolia in the Late Oligocene–Early Miocene (Seyitoğlu and Scott, 1992). The Early–Middle Miocene volcanic rocks of northwestern Anatolia are enriched in LILEs and LREEs relative to HFSEs (negative Ta and Nb anomalies), implying effects of enrichment of the magma source by a subduction component (Aldanmaz et al., 2000).

The Rb/Y vs. Nb/Y diagram (Fig. 10) implies that the features of subduction-related magmas from the trachytes are much higher than in phonolites. These variations may be attributed to the decreasing role of the subducted component in the phonolites. These alkaline volcanics are compared with the Oglakci Miocene volcanics (Temel, 2001) about 30 km east of the studied area, on a Rb/Y–Nb/Y diagram. The trachytes from both regions show subduction-zone enrichment or crustal contamination, but the Nb/Y ratios of the phonolites are higher than in the

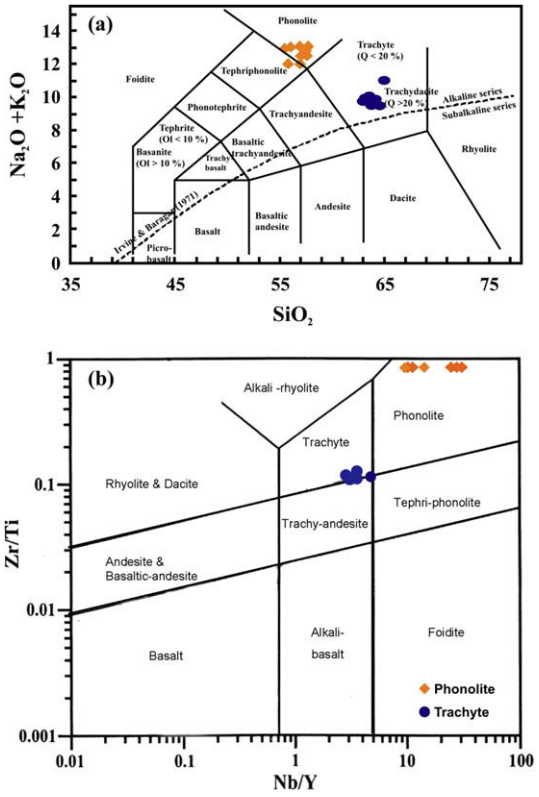

Fig. 7. (a) The distribution of alkaline volcanics in $Na_2O + K_2O$ vs. SiO_2 diagram (after Le Maitre et al., 1989); (b) The position of alkaline volcanics in Zr/Ti–Nb/Y diagram (after Pearce, 1996). (See above-mentioned references for further information.)

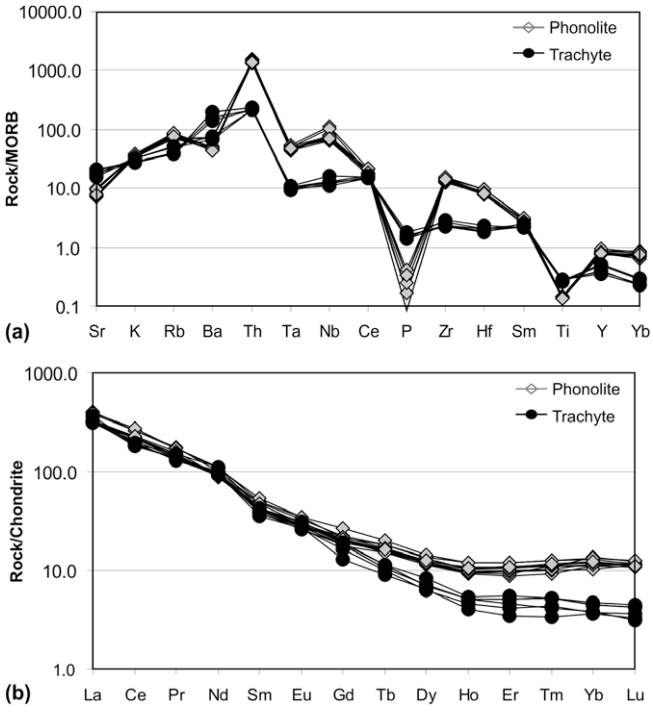

Fig. 8. (a) MORB-normalized spider diagrams of the phonolites and trachytes (normalizing values from Pearce, 1983); (b) Chondrite – normalized REE patterns of the phonolites and trachytes (normalizing values are from Nakamura, 1974).

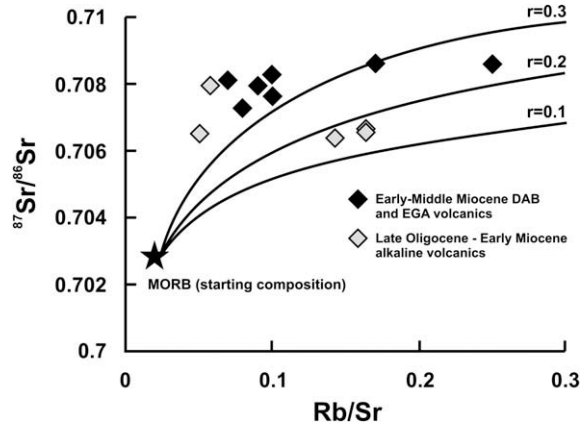

Fig. 9. Rb/Sr vs. $^{87}Sr/^{86}Sr$ diagram for AFC modeling. Variations in r (the ratio of the rate of assimilation/rate of crystallisation) are shown with tick marks. Starting composition (MORB): Sr = 120 ppm, Rb = 2 ppm (Pearce, 1983), $^{87}SR/^{86}Sr = 0.7028$ (Ito et al., 1987; Güleç, 1991).

trachytes, showing parallel direction to a within-plate, enrichment-level–related extensional system. Although the studied area lacks active subduction, the magma source of alkaline rocks with melt enrichment and a within-plate trend is most probably derived from a lithospheric mantle enriched by fluids inherited from pre-collision subduction events (Sarifakioglu, 2006). The alteration of some clinopyroxene crystals to hastingsites in the phonolites may indicate that residual water enriched the melt caused in forming the alkaline volcanic rocks. The enrichment levels of the trachytes in Ba and Sr are higher than in the phonolites, showing similar features in Ni and Co elements. The latter trace elements are thought to have been inherited from a lithospheric mantle source enriched by a subduction component that recorded the previous subduction events. Also, the ophiolites cut by the alkaline volcanics may be attributed to the relicts overthrusted onto the continental platforms of the subducted component resulting from the collision between Pontides and the

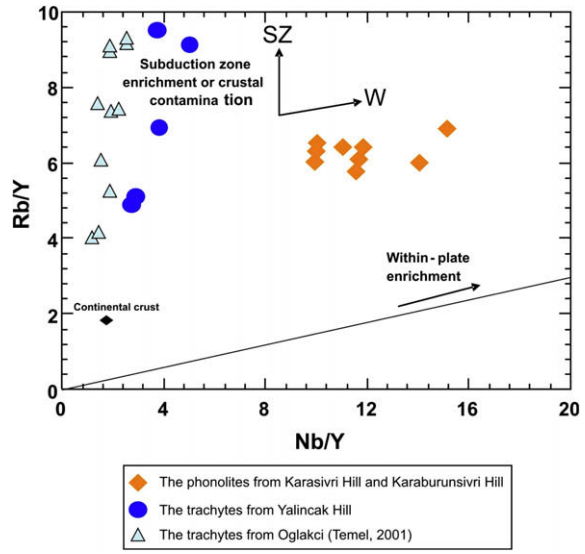

Fig. 10. Rb/Y vs. Nb/Y diagram for the alkaline volcanics (the crustal compositions are from Taylor and McLennan, 1985).

Anatolide–Tauride Platform during the Late Paleocene–Early Eocene.

5.1.3. The role of slab-derived fluids in the geodynamic evolution of Northwestern Anatolia volcanics

Ophiolitic rocks represent the northern branch of the Neo-Tethyan Ocean, cropping out of the Karaburhan surroundings about 20 km northwest of Sivrihisar. The phonolite and trachyte domes cut through peridotites belonging to the ophiolite series. The alkaline domes with high LILE (Th, Ba, Rb, K) values, low Nb, Ta abundances, and LREE enrichment relative to HREE indicate that the phonolites and trachytes mainly originated from a mantle source that was modified by subduction-released fluids. The high Nb/Y ratios (1.3–14.5), low Zr/Nb ratios (2.10–5.88), and low Ce/Pb ratios (<2.5) of the extension-related alkaline volcanics suggest that these rocks were probably affected by hydrous fluids in the filtrate from the previously subducted slab source. However, the high $^{87}Sr/^{86}Sr$ (0.706358–0.708052) and low $^{143}Nd/^{144}Nd$ (0.512546–0.512646) isotope concentrations of the alkaline lavas reflect that the mantle source underwent metasomatism by fluids produced in the source region, which had a subduction component. Their high Pb contents and Pb isotopic compositions are related to the contamination processes resulting from contamination with crustal material during the rise of the alkaline lavas through the thickened lithosphere (over 50 km) in an extensional setting.

In the Galatia Volcanic Province in northwestern Anatolia situated 80 km north of the investigated area, Early Miocene trachyandesites and trachydacites were derived from a mantle source metasomatically enriched by fluids above a subduction zone; however, the Late Miocene alkali basalts formed from the asthenospheric mantle (Wilson et al., 1997). The Late Oligocene–Early Miocene alkaline volcanics were compared with the Miocene Oglakci trachytes (Temel, 2001) about 30 km east of the studied area, showing subduction-zone enrichment or crustal contamination. Similarly, the Late Cenozoic volcanics of the Biga Peninsula were formed from a metasomatized mantle source, but the Quaternary Kula alkali basalts in western Anatolia have OIB-type trace element patterns (Ercan et al., 1995; Aldanmaz et al., 2000; Alıcı et al., 2002).

The alkaline lavas moved through the E–W trending fault lines developing in the local pull-apart basins created by the reactivation of the overthrust line, and through strike-slip faults linked to the extensional regime (Sarifakioglu et al., 2006). In the studied area, the time interval between the thrusting of the Upper Cretaceous ophiolite and the Late Oligocene–Early Miocene alkaline magmatism was not more than 40 Ma. Similarly, the time interval between the collision of the microcontinents along the IAESZ and the other volcanism related to the extension within the Anatolian Plate is considered to be about 30–40 Ma (Harris et al., 1994; Genç and Yılmaz, 1997).

In the western prolongation of the IAESZ in the Vardar suture zone within the Rhodope orogenic belt, an extensional regime prevailed during the Late Eocene–Oligocene (Burg et al., 1990; Pe-Piper and Piper, 2001), whereas along the IAESZ in N–NW Anatolia, the extensional regime only started during the Late Oligocene–Early Miocene (Seyitoğlu and Scott, 1992). As in eastern Anatolia, the first volcanic activity linked to the extension was initiated during the Late Miocene (Keskin, 2003). The studied phonolites and trachytes from the Sivrihisar (Eskisehir) region coincide with a time span during which the extension-related volcanism becomes younger from west to east.

6. Conclusions

The available geological, geochronological, whole-rock, microprobe, and isotope geochemical data from the alkaline volcanics in the Karaburhan (Sivrihisar–Eskisehir) surroundings lead to the following conclusions:

(1) The alkaline volcanics, namely phonolites and trachytes, cut through the already obducted ophiolitic rocks and are parallel to the overthrust line within the IAESZ. The alkaline lavas injected E–W trending faults in an extensional setting formed by the strike-slip movements related to the activation of the overthrust line during the Late Oligocene–Early Miocene.
(2) The mineral assemblages of the phonolites are sanidine, clinopyroxene, feldspathoid (nepheline, hauyne, interstitial analcime), hastingsite, apatite, and Fe–Ti oxide in the hyalo-microlitic porphyritic and fluidal textures; the trachytes mainly consist of fine-grained feldspar and augite crystals in the microlitic fluidal texture.
(3) The alkaline volcanic rocks exhibit negative anomalies in Nb and Ta but enrichment in LILEs and LREEs relative to the MORB. However, the phonolites and trachytes are depleted in HREEs. The alkaline rocks are likely to have been generated from the enriched/metasomatized lithospheric mantle source by the subduction-derived fluids. The existence of hydrous minerals (e.g., hastingsite) in the alkaline rocks may be an indication of such a metasomatism. We interpret the peridotites cut by the alkaline rocks as overthrusted relicts of lithospheric mantle, considered as a main part of SSZ-type ophiolites related to the pre-collision subduction events (Sarifakioglu et al., 2006).
(4) The high $^{87}Sr/^{86}Sr$ (0.706358–0.708052) and low $^{143}Nd/^{144}Nd$ (0.512546–0.512646) isotope concentrations indicate a mantle source enriched by subduction components. The low εNd values, high Pb contents, and Pb isotopic compositions may be related to contamination with crustal material during the rise of the alkaline lavas through the thickened crust (over 50 km).
(5) Late Oligocene–Early Miocene alkaline volcanic rocks display a ratio of assimilation to fractional crystallization ranging from 0.2 to 0.3, affecting their evolution. In western Anatolia and the Aegean region, almost identical results were found for rocks of the same age with $\varepsilon_{Nd} \sim -1$ and $r = \sim 0.3$ (Aldanmaz et al., 2000; Pe-Piper and Piper, 2001; Dilek and Altunkaynak, 2007).

Acknowledgements

Financial support for this study was provided by MTA (The General Directorate of Mineral Research and Exploration) Research Grant 2001-16AE. We would like to thank Ursula Robert for the microprobe analyses and John A. Winchester and Peter A. Floyd for their constructive comments. The valuable and constructive reviews by Boris Litvinovsky, Tom Andersen, and an anonymous reviewer are gratefully acknowledged. The authors thank Bor-ming Jahn for his help to improve the manuscript.

Appendix A

Table A1. The Ar–Ar age data for the four phonolites.

s11a	Mass=	1	J=	9.99E−04	+/−	1.69E−06	Tot. gas. age=	24.578	+/−	0.08				
S11a P1 phonolite/ sanidine	F39	LasPowmW	Vol36	Err36	Vol37	Err37	Vol38	Err38	Vol39	Err39	Vol40	Err40	Age (Ma)	AgeErr
	0.003913	100	6.79969	0.1362	−0.22875	0.13388	1.44312	0.0867	12.49363	0.11491	2232.45	2.40022	31.898	5.72
	0.032809	200	11.79005	0.12516	0.78653	0.11016	2.83546	0.08462	92.24843	0.24175	4419.686	2.87927	18.185	0.719
	0.078105	300	4.51061	0.13304	1.30018	0.14082	1.52214	0.10293	144.6077	0.25912	2978.894	2.4141	20.394	0.487
	0.110333	400	2.56575	0.09128	0.71437	0.1288	0.83545	0.07332	102.8881	0.47473	2155.432	2.15522	24.305	0.481
	0.145042	500	3.86484	0.11263	1.18455	0.19966	1.15628	0.07718	110.8057	0.36885	2706.481	2.77366	25.262	0.542
	0.205766	600	2.64094	0.07071	2.14694	0.19793	1.24238	0.09046	193.8615	0.70899	3580.331	2.80911	25.838	0.215
	0.245873	800	1.45019	0.12346	3.52272	0.21015	0.72423	0.13066	128.0415	0.44016	2210.34	2.07891	24.901	0.514
	0.325708	1000	3.58386	0.08705	0.86788	0.14093	1.53525	0.07757	254.8738	0.39571	4600.053	3.60634	24.861	0.185
	0.514274	1200	10.45457	0.13497	1.73741	0.17872	4.01136	0.10982	601.9934	0.89052	11423.99	2.71476	24.776	0.124
	0.672482	1600	11.12303	0.1309	1.74019	0.21968	3.43242	0.1776	505.0799	1.35025	10238.47	7.59554	24.63	0.153
	0.759251	2000	7.15446	0.11013	1.0239	0.18604	2.20772	0.11043	277.0085	1.04647	5971.793	2.89123	24.919	0.23
	0.986294	3000	9.31556	0.07772	2.73723	0.19049	3.73895	0.13125	724.8318	0.96108	13007.31	6.5722	25.313	0.067
	1	4000	1.2116	0.06959	0.26369	0.21446	0.4978	0.11446	43.75678	0.42329	916.5299	1.00881	22.853	0.866
s11b	Mass=	1	J=	9.99E−04	+/−	1.69E−06	Tot. gas. age=	24.53	+/−	0.106				
S11b P1 phonolite/ sanidine	F39	LasPowmW	Vol36	Err36	Vol37	Err37	Vol38	Err38	Vol39	Err39	Vol40	Err40	Age (Ma)	AgeErr
	0.012708	100	2.32687	0.06818	−0.13198	0.18041	0.46454	0.07463	25.86659	0.24222	988.0792	1.32816	20.811	1.404
	0.073275	200	3.99114	0.09062	0.03202	0.20012	1.04793	0.07054	123.2816	0.47761	2724.881	2.4584	22.448	0.398
	0.13885	300	1.70831	0.06408	0.40674	0.2021	0.46536	0.11566	133.4747	0.58532	2401.604	1.16488	25.426	0.276
	0.196338	400	1.26316	0.06385	0.78504	0.19934	0.53733	0.08376	117.0159	0.46029	2009.45	1.65227	25.02	0.304
	0.235404	500	0.91278	0.09107	0.35461	0.16894	0.54373	0.07327	79.51655	0.54606	1347.504	1.82749	24.258	0.625
	0.265256	600	0.51277	0.08568	0.53378	0.20356	0.58	0.0797	60.76198	0.33503	973.7	1.60968	24.217	0.754
	0.311949	800	0.844	0.08037	0.68953	0.29105	0.73883	0.10485	95.04262	0.32273	1523.847	1.64301	24.001	0.453
	0.382537	1000	1.37165	0.15664	0.50602	0.17391	0.87749	0.1295	143.6781	0.23886	2307.093	2.53968	23.693	0.575
	0.562348	1200	4.05758	0.07217	1.36316	0.20113	2.20832	0.09853	365.9987	0.90515	6236.282	3.46214	24.63	0.121
	0.999599	1600	15.68444	0.20904	3.3814	0.20747	6.68523	0.19445	890.0072	0.62358	17088.17	7.53272	25.037	0.125
	0.999493	2000	0.03497	0.09108	0.21334	0.15155	−0.02186	0.06063	−0.21567	0.1029	−1.72152	0.63746	97.998	217.841
	0.999436	3000	0.07853	0.06165	0.10188	0.15368	0.07263	0.06001	−0.11691	0.10068	−1.13388	0.7051	340.782	354.441
	1	4000	0.10115	0.07925	0.09551	0.11945	0.00831	0.06718	1.14812	0.09895	20.46029	0.68775	−14.861	37.093
s12a	Mass=	1	J=	9.75E−04	+/−	2.29E−06	Tot. gas. age=	24.201	+/−	0.079				
S12a P2 phonolite/ sanidine	F39	LasPowmW	Vol36	Err36	Vol37	Err37	Vol38	Err38	Vol39	Err39	Vol40	Err40	Age (Ma)	AgeErr
	0.003186	100	3.42836	0.13944	0.50842	0.13262	0.70227	0.08382	15.61947	0.16897	1309.858	0.94428	33.124	4.572
	0.025341	200	9.17926	0.10524	0.88405	0.16278	2.1855	0.07957	108.6262	0.44544	3774.188	1.98947	17.115	0.505
	0.064867	300	6.10611	0.16501	1.51054	0.12103	1.86967	0.12055	193.7995	0.49949	4055.484	2.9482	20.322	0.442
	0.095126	400	1.59713	0.07671	0.93175	0.16094	0.72489	0.09168	148.3634	0.67702	2438.65	1.28463	23.173	0.286
	0.120955	500	1.43546	0.11754	0.98196	0.12703	0.6109	0.0855	126.639	0.26787	2192.16	1.33506	24.397	0.479
	0.177851	600	1.86995	0.07678	2.5161	0.19928	1.17097	0.12403	278.962	0.90848	4506.113	3.25699	24.764	0.164
	0.233946	800	1.37513	0.10877	1.95394	0.13473	0.97351	0.14058	275.0352	0.83666	4233.731	2.86345	24.319	0.217
	0.291278	1000	3.04339	0.07863	1.3614	0.16526	1.45101	0.14371	281.1015	0.72106	4730.709	4.09896	23.822	0.158
	0.385696	1200	4.68165	0.16137	1.67389	0.19593	2.1339	0.15868	462.9347	1.00131	7764.018	6.85278	24.088	0.188
	0.537392	1600	10.48691	0.14208	3.35297	0.20959	4.39649	0.10641	743.7724	0.87277	13455.23	4.71109	24.333	0.103
	0.543267	2000	0.2485	0.05349	0.12572	0.10239	0.12094	0.06905	28.80434	0.20117	504.2547	1.27537	26.125	0.972
	0.972445	3000	26.50375	0.2813	14.71412	0.27611	9.42024	0.26115	2104.277	2.92606	37722.72	12.59868	24.82	0.077
	1	4000	2.4978	0.12187	0.33958	0.10734	0.87409	0.09131	135.105	0.23397	2620.108	1.72548	24.343	0.465

(continued on next page)

Table A1 (*continued*)

s12b	Mass=	1	*J*=	9.75E−04	+/−	2.29E−06	Tot. gas. age=	24.35	+/−	0.119				
S12b P2 phonolite/ sanidine	F39	LasPowmW	Vol36	Err36	Vol37	Err37	Vol38	Err38	Vol39	Err39	Vol40	Err40	Age (Ma)	AgeErr
	0.001934	100	1.10788	0.05898	−0.16915	0.17407	0.22676	0.0655	4.07399	0.14321	442.4171	1.37498	49.009	7.543
	0.018297	200	2.31372	0.05834	−0.0737	0.27586	0.50852	0.07879	34.46066	0.27345	1135.393	1.54769	22.915	0.891
	0.057333	300	3.15839	0.06214	0.15627	0.18374	0.64466	0.03581	82.2124	0.41482	1877.487	2.25283	20.094	0.404
	0.099637	400	0.77189	0.10029	0.31089	0.16428	0.49941	0.05933	89.09647	0.53409	1477.374	1.88456	24.503	0.597
	0.136586	500	2.37907	0.09096	0.45308	0.18378	0.76932	0.10227	77.8183	0.44339	1849.002	2.00007	25.725	0.618
	0.208886	600	4.40404	0.08342	1.51989	0.17116	1.75339	0.0964	152.2704	0.48051	3405.004	2.78308	24.144	0.293
	0.257407	800	1.70371	0.04489	0.71872	0.14548	1.00486	0.08564	102.1889	0.36568	1933.728	1.99953	24.459	0.244
	0.293728	1000	1.59807	0.09143	0.24771	0.11881	0.95499	0.08103	76.4952	0.28863	1518.069	2.09267	23.895	0.622
	0.347977	1200	4.26109	0.07371	−0.00884	0.09243	1.27988	0.09677	114.2531	0.50211	2909.702	1.50526	25.24	0.349
	0.5661	1600	13.72853	0.20193	1.6219	0.35893	4.70477	0.12812	459.384	0.79016	10372.52	4.91579	24.028	0.23
	1.000022	2000	30.78714	0.27089	1.88919	0.17136	9.72927	0.22201	913.8769	1.70044	21927.85	5.53404	24.533	0.159
	0.999967	3000	−0.06704	0.07189	−0.03884	0.13089	0.04165	0.08851	−0.11609	0.07675	0.28009	0.5448	−333.512	456.903
	1	4000	−0.13937	0.0536	−0.16196	0.09847	0.08889	0.08666	0.06938	0.12632	1.40599	0.53425	846.419	1255.53

References

Aldanmaz, E., Pearce, J.A., Thirwall, M.F., Mitchell, J.G., 2000. Petrogenetic evolution of Late Cenozoic post-collision volcanism in western Anatolia, Turkey. Journal of Volcanology and Geothermal Research 102, 67–95.

Alıcı, P., Temel, A., Gourgaud, A., 2002. Pb–Nd–Sr isotope and trace element geochemistry of Quaternary extension-related alkaline volcanism: a case study of Kula region (western Anatolia, Turkey). Journal of Volcanology and Geothermal Research 115, 487–510.

Bingöl, E., 1976. The geotectonic evolution of western Anatolia. Mineral Research and Exploration Institute of Turkey (MTA) Publication 86, 4–34 (in Turkish).

Bingöl, E., Akyürek, B., Korkmazer, B., 1973. The geology of Biga Peninsula and some features of Karakaya Formation. In: Proceedings of the Earth Sciences Congress of the 50th Anniversary Turkish Republic, pp. 70–76 (in Turkish).

Burg, J.P., Ivanov, Z.., Ricou, L.E., Dimor, D., Klain, L., 1990. Implications of shear-sense criteria for the tectonic evolution of the Central Rhodope massif, southern Bulgaria. Geology 18, 451–474.

DePaolo, D.J., 1981. Trace element and isotopic effects of combined wall rock assimilation and fractional crystallization. Earth and Planetary Scientific Letters 53, 189–202.

Dilek, Y., Altunkaynak, S., 2007. Cenozoic crustal evolution and mantle dynamics of post-collisional magmatism in Western Anatolia. International Geology Review 49, 431–453.

Edwards, C., Menzies, M., Thirlwall, M., 1991. Evidence from Muriah, Indonesia, for the interplay of supra-subduction zone and intraplate processes in genesis of potassic alkaline magmas. Journal of Petrology 32 (3), 555–592.

Ercan, T., Satır, M., Steinitz, G., Dora, A., Sarıfakıoğlu, E., Adis, C., Walter, H.J., Yıldırım, T., 1995. The features of Tertiary volcanism from Biga Peninsula, Gökçeada, Bozcaada and Tavsan islands (NW Anatolia). Mineral Research and Exploration Institute of Turkey (MTA) Publications 117, 55–86 (in Turkish).

Fitton, J.G., James, D., Kempton, P.D., Ormerod, D.S., Leeman, W.P., 1998. The role of lithospheric mantle in the generation of Late Cenozoic Basic Magmas in the western United States. Journal of Petrology. Special Lithosphere Issue, 331–349.

Genç, Ş.C., Yılmaz, Y., 1997. An example of post-collisional magmatism in Northwestern Anatolia: the Kızderbent volcanics (Armutlu peninsula, Turkey). Turkish Journal of Earth Sciences 6, 33–42.

Göncüoğlu, M.C., Turhan, N., Şentürk, K., Özcan, A., Uysal, Ş., Yalınız, K., 2000. A geotraverse across northwestern Turkey: tectonic units of the Central Sakarya region and their tectonic evolution. In: Bozkurt, E., Winchester, J.A., Piper, J.D.A. (Eds.), Tectonics and Magmatism in Turkey and Surrounding Area, Special Publications 173. Geological Society, London, pp. 137–161.

Gözler, M.Z., Cevher, F., Ergül, E., Asutay, H.J., 1996. The geology of Central Sakarya and its southern part. MTA Report No: 9973 (unpubl.) (in Turkish).

Güleç, N., 1991. Crust–mantle interaction in Western Turkey: implications from Sr and Nd isotope geochemistry of Tertiary and Quaternary volcanics. Geological Magazine 128, 417–435.

Hall, C.M., Farrell, J.W., 1995. Laser 40Ar/39Ar ages of tephra from Indian Ocean deep-sea sediments: tie points for the astronomical and geomagnetic polarity time scales. Earth and Planet Science Letters 133, 327–338.

Harris, N.B.W., Kelley, S., Okay, A.I., 1994. Post-collision magmatism and tectonics in northwest Anatolia. Contributions to Mineralogy and Petrology 117, 241–252.

Hart, S.R., Erlank, A.J., Kable, E.J.D., 1974. Sea floor basalt alteration: some chemical and Sr isotopic effects. Contribution of Mineralogy and Petrography 44, 219–230.

Hatzle, T., 1992. Die Genese Der Karbonatit-und Alkalivulkanit-Assoziierten Fluorit-Baryt-Bastnasit-Vererzung Bei Kızılcaören (Turkei). Münchner Geol. Hefte. Technischen Universitat München, 271 pp.

Humphris, S.E., Thompson, G., 1978. Trace element mobility during hydrothermal alteration of oceanic basalts. Geochimica et Cosmochimica Acta 42, 127–136.

Irvine, T.N., Baragar, W.R.A., 1971. A guide to the chemical classification of the common volcanic rocks. Journal Earth Science Canada 8, 523–548.

Ito, E., White, W.M., Göpel, C., 1987. The O, Sr, Nd and Pb isotope geochemistry. Chemical Geology 62, 157–176.

Keskin, M., 2003. Magma generation by slab steepening and breakoff beneath a subduction-accretion complex: an alternative model for collision-related volcanism in Eastern Anatolia, Turkey. Geological Research Letters 30. doi:10.1029/2003GL018019.

Le Pichon, X., Angelier, J., 1979. The Hellenic arc and trench system: a key to the neotectonic evolution of eastern Mediterranean area. Tectonophysics 60, 1–42.

Le Maitre, R.W., Baterman, P., Dudek, A., Keller, J., Lameyre Le Bas, M.J., Sabine, P.A., Schmid, R., Sorensen, H., Streckeisen, A., Woolley, A.R., Zannettin, B., 1989. A Classification of Igneous Rocks and Glossary of Terms. Blackwell, Oxford.

McKenzie, D., 1978. Active tectonics of the Alpine-Himalayan belt: the Aegean sea and surrounding regions. Geophysical Journal of the Royal Astronomical Society 55, 217–254.

Monod, O., Andrieux, J., Gautler, Y., Kienast, J.R., 1991. Pontides–Taurides relationships in the region of Eskisehir (NW Turkey). Bulletin of the Technical University Istanbul 44, 257–278.

Nakamura, N., 1974. Determination of REE, Ba, Fe, Mg, Na and K in carbonaceous and ordinary chondrites. Geochimica et Cosmochimica Acta 38, 757–775.

Norman, M.D., Garcia, M.O., 1999. Primitive magmas and source characteristics of the Hawaiian plume: petrology and geochemistry of shield picrites. Earth and Planet Science Letters 168, 27–44.

Okay, A.I., 1984. Distribution and Characteristics of the Northwest Turkish Blueschists, Special Publications 17. Geological Society, London. pp. 455–466.

Okay, A.I., Siyako, M., Bürkan, K.A., 1990. The geology of Biga Peninsula and its tectonic evolution. Bulletin of TPJD 1 (3), 83–121 (in Turkish).

Okay, A.I., Tansel, İ., Tüysüz, O., 2001. Obduction, subduction and collision as reflected in the Upper Cretaceous–Lower Eocene sedimentary record of western Turkey. Geological Magazine 138, 117–142.

Okay, A.I., Tüysüz, O., 1999. Tethyan sutures of northern Turkey. In: Durand, B., Jolivet, L., Horvath, F., Serrane, M. (Eds.), The Mediterranean Basins: Tertiary Extension within the Alpine Orogen, Special Publications 156. Geological Society, London, pp. 475–515.

Ozen, H., Sarifakioglu, E., 2003. The petrographical and petrological features of volcanites in the Sivrihisar (Eskisehir) vicinity. In: 56th Turkish Geology Congress. Abstracts, pp. 20–21 (in Turkish).

Özgenç, İ., 1993. Geology and REE geochemistry of carbothermal bastnaesite-fluorite-baryte deposit of Kizilcaoren (Sivrihisar, Eskisehir). Geological Bulletin of Turkey 36, 1–11 (in Turkish).

Pearce, J.A., 1983. Role of the subcontinental lithosphere in magma genesis at active continental margins. In: Hawkesworth, C.J., Norry, M.J. (Eds.), Continental Basalts and Xenoliths. Shiva Publishing, Cheshire, pp. 230–249.

Pearce, J.A., 1996. A users guide to basalt discrimination diagrams. In: Wyman, D.A. (Ed.), Trace Element Geochemistry of Volcanic Rocks: Applications for Massive Sulphide Exploration. Geochemistry Short Course Notes, vol. 12. Geological Association of Canada, pp. 79–113.

Pe-Piper, G., Piper, D.J.W., 2001. Late cenozoic, post-collisional Aegean igneous rocks: Nd, Pb and Sr isotopic constraints on petrogenetic and tectonic models. Geological Magazine 138, 53–668.

Renne, P.R., Swisher, C.C., Deino, A.L., Karner, D.B., Owens, T.L., DePaolo, D.J., 1998. Intercalibration of standards, absolute ages, and uncertainties in $^{40}Ar/^{39}Ar$ dating. Chemical Geology 145, 117–152.

Samson, S.D., Alexander, E.C., 1987. Calibration of the interlaboratory $^{40}Ar/^{39}Ar$ dating standard, Mmhb-1. Chemical Geology 66, 27–34.

Sarifakioglu, E., 2006. Petrology and origin of plagiogranites from the Dagkuplu (Eskisehir) ophiolite along the Izmir-Ankara-Erzincan suture zone, Turkey. Ofioliti 32, 39–51.

Sarifakioglu, E., Ozen, H., Colakoglu, A.O., Sayak, H., 2006. An new approach to the petrogenesis and age of alkaline volcanites cut through the Dagkuplu Ophiolite (Sivrihisar, Eskisehir), NW Anatolia. Bulletin of the Mineral Research and Exploration Institute (MTA), Turkey 132, 75–90 (in Turkish).

Seyitoğlu, G., Scott, B.C., 1992. Late Cenozoic volcanic evolution of the NE Aegean region. Journal of Volcanology Geothermal Research 54, 157–176.

Sun, S.S., McDonough, W.F., 1989. Chemical and isotopic systematics of oceanic basalts: implications for mantle composition and processes. In: Saunders, A.D., Norrl, M.J. (Eds.), Magmatism in the Ocean Basins, Special Publication 42. Geological Society, London, pp. 313–345.

Şengör, A.M.C., Yılmaz, Y., 1981. Tethyan evolution of Turkey: a plate tectonic approach. Tectonophysics 75, 181–241.

Şengör, A.M.C., Satır, M., Akkök, R., 1984. Timing of tectonic events in the Menderes Massif, western Turkey: implications for tectonic evolution and evidence for Pan-African basement in Turkey. Tectonics 3, 603–707.

Taylor, S.R., McLennan, S.M., 1985. The Continental Crust: Its Composition and Evolution. Blackwell Scientific Publications, Oxford, UK. 312 pp.

Temel, A., 2001. Post-collision Miocene alkaline volcanism in the Oglakçi Region, Turkey: petrology and geochemistry. International Geology Review 43, 640–660.

Türkecan, A., Kuzucuoğlu, C., Mouralis, D., Pastre, J.-F., Atıcı, Y., Guillou, H., Fontugne, M., 2004. Upper pleistocene volcanism and palaegeography in Cappadocia, Turkey. MTA-CNRS-TUBITAK 2001-2003 Research Programme. Tubitak Project No: 101Y109; MTA Report No: 10652. 180pp.

Wilson, M., Tankut, A., Güleç, N., 1997. Tertiary volcanism of the Galatia province, north-west Central Anatolia, Turkey. Lithos 42, 105–121.

Yılmaz, Y., 1990. Comparisons of young volcanic association of western and eastern Anatolia formed under a compressional regime: a review. Journal of Volcanology and Geothermal Research 44, 69–87.

Zindler, A., Hart, S.R., 1986. Chemical geodynamics. Annual Review of Earth and Planet Science Letters 14, 493–571.